Article ID: 1000-324X(2019)12-1341-08 **DOI:** 10.15541/jim20190121

Fabrication and Property of Yb:CaF_2 Laser Ceramics from Co-precipitated Nanopowders

WEI Jia-Bei[1,2], TOCI Guido[3], PIRRI Angela[4], PATRIZI Barbara[5], FENG Ya-Gang[1,2], VANNINI Matteo[3], LI Jiang[1,2]

(1. Key Laboratory of Transparent Opto–Functional Inorganic Materials, Shanghai Institute of Ceramics, Chinese Academy of Sciences, Shanghai 200050, China; 2. Center of Materials Science and Optoelectronics Engineering, University of Chinese Academy of Sciences, Beijing 100049, China; 3. Istituto Nazionale di Ottica, Consiglio Nazionale delle Ricerche, CNR-INO, 50019 Sesto Fiorentino (Fi), Italy; 4. Istituto di Fisica Applicata "Carrara", Consiglio Nazionale delle Ricerche, CNR-IFAC, 50019 Sesto Fiorentino (Fi), Italy; 5. Istituto Nazionale di Ottica, Consiglio Nazionale delle Ricerche, CNR-INO, 56124 Pisa (Pi), Italy)

Abstract: Transparent ytterbium doped calcium fluoride ceramics (Yb:CaF_2) were successfully fabricated by vacuum sintering and hot pressing post-treatment from coprecipitated powders. In-line transmittance of 5at% Yb:CaF_2 transparent ceramics fabricated by pre-sintering at 600 ℃ for 1 h and hot pressing post-treatment at 700 ℃ for 2 h, reaches 92.0% at the wavelength of 1200 nm. Microstructure, spectroscopic characteristics and laser performance of the ceramics were measured and discussed. The sample shows a homogeneous microstructure with average grain size of 360 nm. Furthermore, the absorption cross section at 977 nm and the emission cross section at the 1030 nm of the ceramics are calculated to 0.39×10^{-20} cm^2 and 0.26×10^{-20} cm^2, respectively. Finally, the laser behavior was tested, finding a maximum output power of 0.9 W while the highest slope efficiency was 23.6%.

Key words: Yb:CaF_2; co-precipitation synthesis; two-step sintering; laser ceramics; optical property

In recent years, solid state lasers have been widely used in many fields, such as inertial confinement fusion, medical science and manufacturing. The gain medium is an important part of the laser system. The common materials used as gain media include glass, transparent ceramics and single crystals. Polycrystalline transparent ceramics have attracted considerable attention over the last few years. Compared with traditional optical glass, transparent ceramics show obvious superiorities on mechanical and thermal property. Generally transparent ceramics exhibit advantages over single crystals in many aspects, such as lower cost in preparation, higher homogeneity of the dopant and larger size[1-4]. Many kinds of transparent ceramics have been studied and great achievements have already been acquired, such as YAG[5-9], sesquioxides[10-15], and fluorides[16-18]. In the case of fluoride ceramics, the current progress of the researches and development fall behind oxide ceramic materials, although the first laser ceramics, Dy:CaF_2, were fabricated by Hatch, *et al* in 1964[19].

Fluoride crystalline hosts, such as CaF_2 and its Sr and Ba based isomorphs (*i.e.* SrF_2 and BaF_2) possess excellent property such as broad range of transmittance, lower phonon energy and low refraction index than garnets and sesquioxides; in these hosts Yb^{3+} features a very broad absorption and emission bands (useful for the generation and amplification of ultrashort laser pulses) and long fluorescence lifetime that ensures efficient energy storage for the laser operation[20-21]. In addition, Yb:CaF_2 has a negative thermo-optical coefficient which is suitable for the high output power in lasers due to mitigation of the thermal lens effect[22-23]. Due to these characteristics, crystalline CaF_2 is a widely used host for efficient Yb doped[20, 24-27] and Nd doped materials for laser applications[28].

The success of crystalline CaF_2 as laser host has stimulated the development of ceramics with the same composition for laser applications, in particular with Yb^{3+} doping[18, 21-22].

A large number of scientific literatures have been published on Yb:CaF_2 transparent ceramics and some progresses have been made. Basiev, *et al*[17, 29-30] successfully fabricated Yb:CaF_2 laser ceramics with high optical quality by the hot forming method and reported the laser operation. But this hot forming method needs corresponding single crystal as the starting material and

Received date: 2019-03-25; **Modified date:** 2019-04-25
Foundation item: National Natural Science Foundation of China (61575212); Key Research Project of the Frontier Science of the Chinese Academy of Sciences (QYZDB-SSW-JSC022)
Biography: WEI Jia-Bei (1993–), male, candidate of Master degree. E-mail: weijiabei@student.sic.ac.cn
Corresponding author: LI Jiang, professor. E-mail: lijiang@mail.sic.ac.cn

therefore it does not have the general advantages of ceramics preparation, such as short sintering time and low fabrication cost. Mortier, *et al*[18, 31-33] has investigated the fabrication of Yb:CaF_2 transparent ceramics by sintering under vacuum atmosphere combined with the hot pressing method and the reported laser oscillation. Li, *et al*[34] prepared Yb:CaF_2 by vacuum hot pressing and spark plasma sintering respectively. In 2015, Aballea, *et al*[35-36] reported the fabrication of Yb:CaF_2 transparent ceramics by sintering at moderate temperature in air and without any pressure assistance; moreover they demonstrated the laser operation of nano-powder based Yb:CaF_2 ceramics. In 2017, Kitajima, *et al*[37] studied Yb, La:CaF_2 transparent ceramics sintered by hot isostatic pressing (HIP) method. They reported the laser operation of the Yb^{3+}- doped CaF_2-LaF_2 ceramics with a maximum output power of 4.36 W and a maximum slope efficiency of 69.5%.

In this study we report on the fabrication, spectroscopic investigation and laser behavior of a 5at% Yb:CaF_2 transparent ceramic obtained by vacuum sintering and hot pressing post-treatment. The nano-powders were synthesized by the co-precipitation method. Then the FT-IR spectrum, phase composition and morphology of these powders were measured. The microstructure and in-line transmittance of the samples were investigated. Meanwhile, the fundamental spectroscopic characteristics of 5at% Yb:CaF_2 transparent ceramics were systematically studied. Finally, we test the laser characteristic of the sample finding encouraging results.

1 Experimental

5at% Yb:CaF_2 nano-scale powders were synthesized by the co-precipitation method. Commercially available chemical reagent included hydrated calcium nitrate (99.90%, Sinopharm Chemical Reagent Co., Ltd., Shanghai, China), hydrated potassium fluoride (99.90%, Sinopharm Chemical Reagent Co., Ltd., Shanghai, China), Ytterbium oxide (99.99%, Alfa Aesar, USA). $Ca(NO_3)_2$ solution and KF solution were prepared by dissolving hydrated calcium nitrate and hydrated potassium fluoride in deionized water, respectively. The $Yb(NO_3)_3$ solution was obtained by dissolving Yb_2O_3 powders in nitric acid at 80 ℃. Then the solutions were filtered to remove the undissolved particles and impurities with 0.3 μm aperture size filter paper. The solution of potassium fluoride was added to the mixed solution of calcium nitrate and yttrium nitrate using a peristaltic pump under magnetic stirring. Next, the obtained solution was aged for 12 h at room temperature. The suspension was washed and centrifuged with deionized water for several times. Subsequently, the washed suspension was dried at 70 ℃ for 48 h in an oven, and the dried powders were sieved through a 74-μm screen. Finally, 5at% Yb:CaF_2 nano-powders were obtained.

The synthesized nano-powders were dry-pressed in a 34 mm diameter die at 20 MPa, followed by cold isostatic pressing (CIP) at 250 MPa. The green body was sintered under vacuum at 600 ℃ for 1 h. Then, the pre-sintered sample was hot pressed at 700 ℃ with 30 MPa pressure under vacuum. The obtained Yb:CaF_2 ceramic sample was polished into 1.5 mm for the further characterizations.

The phase of the powders was determined by X-ray diffraction (XRD, Model D/max2200 PC, Rigaku, Japan) in the range of 2θ between 10° and 80° using nickel-filtered Cu-Kα radiation. Fourier transform infrared spectroscopy (FT-IR) was performed on an infrared spectrometer (FT-IR, Bruker VERTEX 70 spectrophotometer, Ettlingen, Germany) using the standard KBr method in the range of 4000–400 cm^{-1}. The specific surface area (S_{BET}) of the powders was performed by Norcross ASAP 2010 Micromeritics with N_2 as the absorption gas at 77 K. The morphologies of powders and microstructures of the fracture surfaces of ceramics were observed by a scanning electron microscope (FESEM, SU8220, Hitachi, Japan). The absorption intensity and in-line transmittance of the transparent ceramics were measured by a UV-VIS-NIR spectrophotometer (Model Cray-5000, Varian, CA, USA). The emission spectrum excited by a 915 nm laser beam was measured by a low temperature absorption spectrometer (FLS980, Edinburgh Instruments, Edinburgh, UK) at room temperature. The decay curve of the ceramics was measured using a pulsed Ti:Sapphire laser at 900 nm for excitation, using the so-called pinhole method for the correction of the radiation trapping effects[38-39]. The laser emission of 5at% Yb:CaF_2 transparent ceramics was tested in an end pumped cavity, using a fiber coupled diode laser as pumping source.

2 Results and discussion

Fig. 1 shows the FT-IR spectrum of 5at% Yb:CaF_2 powders. The wide absorption band around 3420 cm^{-1} is related to the stretching vibrations of OH^- group. The band around 1644 cm^{-1} corresponds to H–O–H bending mode. Nevertheless, the hygroscopic property of matrix material KBr must be taken into consideration when analyzing the information provided by OH^- and H–O–H vibration band during the measurements, which affects the test results. The absorption peak at 2364 cm^{-1} is caused by the adsorption of CO_2 in the air and provides no information as a consequence. The absorption peak at

1383 cm^{-1} is due to NO_3^- elongation mode. An effective washing process can decrease absorbed nitrate content and impurity ions like K^+ ions in the powders. The residual nitrates and absorbed water in the powders are decomposed during pre-sintering process.

Fig. 2 shows the XRD pattern of 5at% Yb:CaF_2 powders. It can be seen that all diffraction peaks of the powders are well matched with those of the cubic CaF_2 phase (PDF# 35-0816) and no secondary phase can be detected. Meanwhile, all the peaks of the powders shift to a lower angle, which reveals that the lattice parameter increases. This occurs because Yb^{3+} enters into the CaF_2 structure by substituting for a Ca^{2+} and creating an extra F^- for charge compensation; as a consequence, the charge repulsion between F^- ions increases the lattice parameter. The grain size (D_{XRD}) of the powders can be calculated by the Scherrer equation:

$$D_{XRD} = \frac{0.89\lambda}{\beta \cdot \cos\theta} \tag{1}$$

where β is the full width at half-maximum (FWHM) of a diffraction peak at Bragg angle θ and λ is the wavelength of CuKα radiation used in the measurements. The calculated average grain size of 5at% Yb:CaF_2 powders is 32 nm.

Fig. 3(a) shows the SEM micrograph of 5at% Yb:CaF_2 powders. It appears that the powders are well-distributed and slightly agglomerated. The shape of the small particles

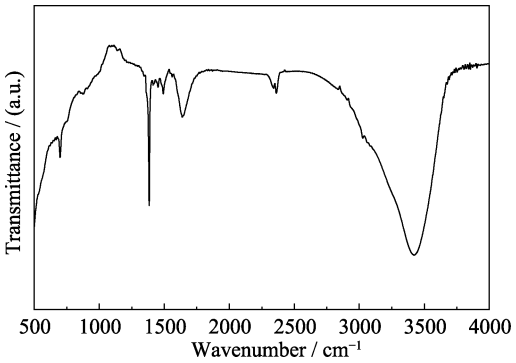

Fig. 1　FT-IR spectrum of 5at% Yb:CaF_2 powders

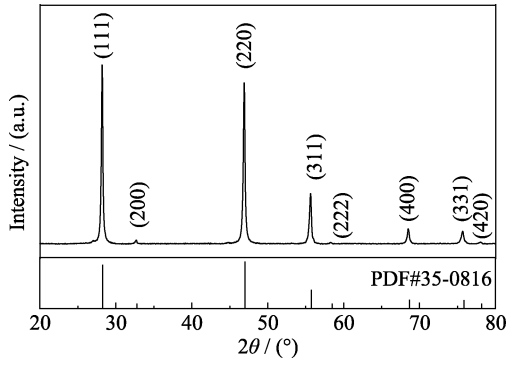

Fig. 2　XRD pattern of 5at% Yb:CaF_2 powders

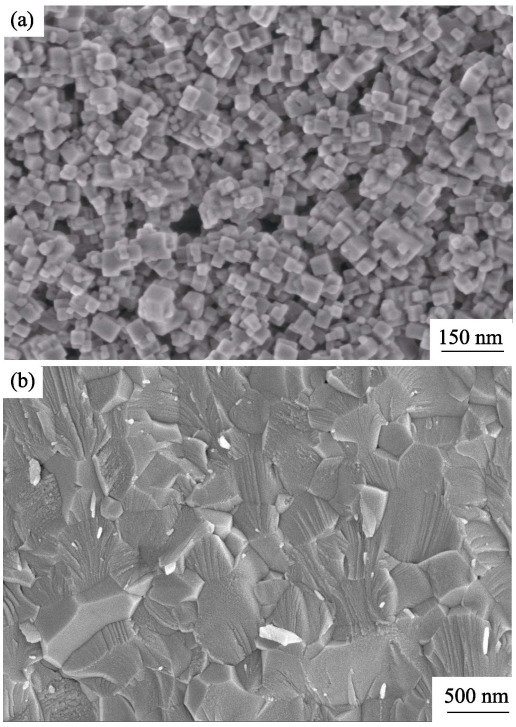

Fig. 3　SEM micrographs of 5at% Yb:CaF_2 powders (a) and the fracture surface of 5at% Yb:CaF_2 ceramics (b)

is close to cubic. The average particle size (D_{BET}) is 45 nm, which is calculated from the following formula

$$D_{BET} = \frac{6}{\rho \cdot S_{BET}} \tag{2}$$

where (ρ=3.473 g/cm^3) is the theoretical density of the powders calculated from their lattice parameters. S_{BET} is the specific surface area determined by BET measurement. Meanwhile, it can be found that the size of 5at% Yb:CaF_2 powders calculated by BET method is larger than the value calculated by the Scherrer equation, indicating the existence of weak agglomerates, which can be observed from SEM micrograph of the powders.

Fig. 3(b) shows the SEM micrograph of the fracture surface of 5at% Yb:CaF_2 transparent ceramics fabricated by vacuum pre-sintering at 600 ℃ for 1 h and hot pressing at 700 ℃ for 2 h. It reveals that the ceramics have an homogeneous structure and the average grain size is about 360 nm. The fracture mode is mainly transgranular. Moreover, it can be observed that some residual pores exist at the grain boundaries. It is known that these residual pores cause scattering loss in the transparent ceramics, which can decrease their optical quality. The work in future will focus on the complete elimination of the residual pores by HIP post-treatment.

The in-line transmittance and the photograph of 5at% Yb:CaF_2 transparent ceramics are shown in Fig. 4. As it can be seen in the inset of Fig. 5, the size of ceramics is 16 mm×6.8 mm while the thickness is 1.5 mm. At a visual inspection, ceramics have good transparency and the

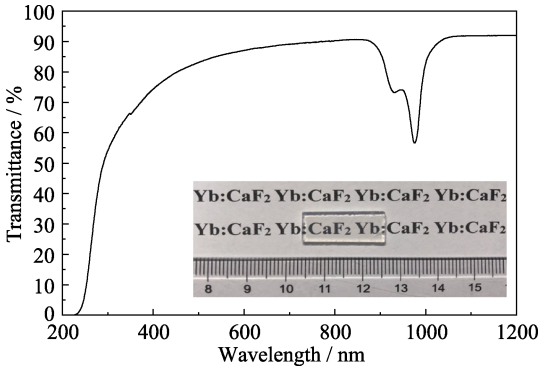

Fig. 4 The in-line transmittance and the photograph of 5at% Yb:CaF_2 transparent ceramics

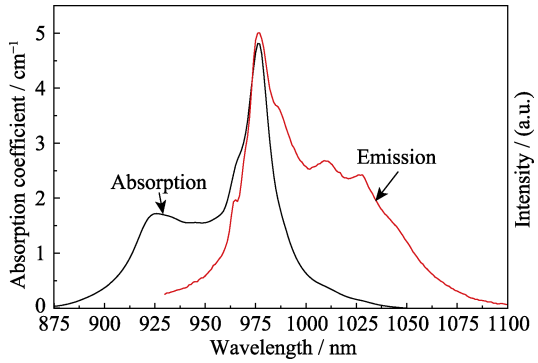

Fig. 5 Absorption coefficient and emission spectra of 5at% Yb:CaF_2 transparent ceramics at room temperature

letters on the underlying paper can be clearly recognized.

According to Krell[40], without scattering or absorption losses, the theoretical maximum of transmission is 100% minus reflection on both surfaces of a window. At normal incidence, the reflection R_1 on one surface is governed by the refractive index n as:

$$R_1 = \left\{\frac{n-1}{n+1}\right\}^2 \tag{3}$$

And the total reflection loss (including multiple reflection) is:

$$R_2 = \frac{2R_1}{1+R_1} \tag{4}$$

Thus, the theoretical limit is:

$$T_{th} = (1-R_2) = \frac{2n}{n^2+1} \tag{5}$$

It is well known that the refractive index of CaF_2 single crystal decreases as the wavelength increases. At 1200 nm, the un-doped CaF_2 single crystal has a refractive index of 1.4277[41]. Based on the above equation, the theoretical transmittance of CaF_2 single crystal is 93.97% at 1200 nm. The transmittance of 5at% Yb:CaF_2 transparent ceramics we have prepared reaches 92.0%, which is very close to the theoretical value. However, at the wavelength of 400 nm, the transmittance is 74.3%. The transmittance in visible range decreases rapidly, which can be attributed to the residual nanoscale pores in the ceramics.

The room temperature absorption coefficient and emission spectrum of 5at% Yb:CaF_2 transparent ceramics are shown in Fig. 5. The pump source used to excite the sample to measure the emission spectrum is a fiber-coupled laser diode (LD) with center wavelength at 915 nm. It can be seen that the spectrum has broad absorption band. There are two main strong absorption peaks at 925 and 977 nm, corresponding to the transition from the ground state $^2F_{7/2}$ to the excited state $^2F_{5/2}$ of Yb^{3+} ions. The absorption coefficient is calculated by the following equations:

$$R = \left(\frac{1-n}{1+n}\right)^2 \tag{6}$$

$$T = \frac{(1-R)^2 e^{(-\alpha b)}}{1-R^2 e^{(-2\alpha b)}} \tag{7}$$

Where T is the transmittance of the ceramics, α and b are the absorption coefficient and the thickness of the sample, respectively. At 977 nm, the absorption coefficient is 4.8 cm^{-1}, which is suitable for pumping by high powder InGaAs laser diodes. The emission spectrum has a broad emission band, ranging from 960 nm to 1040 nm. The main emission peaks that can be seen are near 977, 1010, 1030 nm, which can be attributed to $^2F_{5/2} \rightarrow {}^2F_{7/2}$ transition of Yb^{3+} ions.

Fig. 6 (a) shows the absorption cross section spectrum of 5at% Yb:CaF_2 transparent ceramics at room temperature.

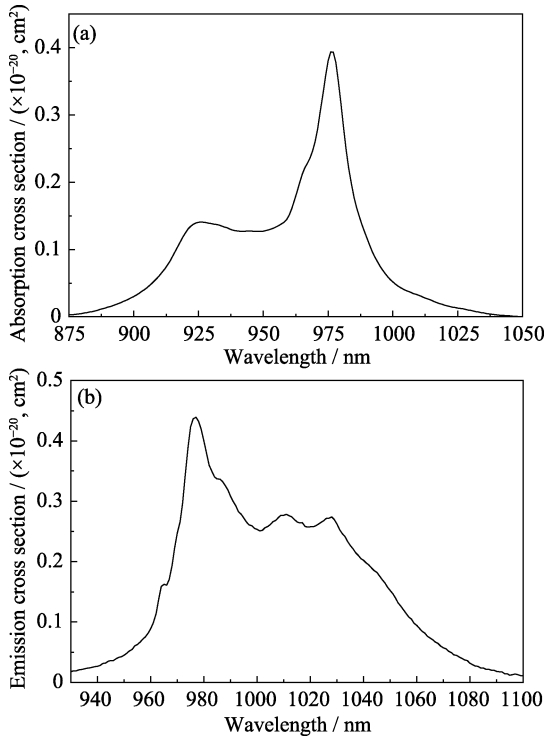

Fig. 6 Absorption cross section spectrum (a) and emission cross section spectrum (b) of 5at% Yb:CaF_2 transparent ceramics at room temperature

The absorption cross section σ_{abs} can be calculated by the following formula:

$$\sigma_{abs} = \frac{\alpha}{N} \tag{8}$$

Where α is the absorption coefficient calculated above; N is the number of the doping ions per unit volume. The absorption cross section at 977 nm is calculated to 0.39×10^{-20} cm^2.

The Fuchtbauer-Ladenburg equation was used to calculate the emission cross section, with the expression of the Eq. (9).

$$\sigma_{em}(\lambda) = \frac{\lambda^5}{8\pi n^2 c\tau_{rad}} \cdot \frac{I(\lambda)}{\int \lambda I(\lambda)\mathrm{d}\lambda} \tag{9}$$

Where c is light speed: 3.0×10^8 m/s; λ is wavelength; n is the refractive index; τ_{rad} is upper level radiation lifetime: 2.4 ms[42]; $I(\lambda)$ is fluorescence intensity at a certain wavelength in the fluorescence spectrum. The emission cross section spectrum of 5at% Yb:CaF_2 transparent ceramics is showed in Fig. 6(b). The value of the emission cross section at the 1030 nm is 0.26×10^{-20} cm^2.

The gain cross section of 5at% Yb:CaF_2 transparent ceramics was calculated by the formula:

$$\sigma_g = \beta\sigma_{em}(\lambda) - (1-\beta)\sigma_{abs}(\lambda) \tag{10}$$

Where β is particle inversion number. The gain cross section with different β are reported in Fig. 7. It can be observed that the gain cross-section curves show wide and flat shapes, which are very helpful to realize broadband tuning and ultra-short pulse laser output.

For the measurement of the upper laser level lifetime, the sample was excited using a pulsed Ti:Sapphire laser emitting at 900 nm with a pulse duration of about 100 ns FWHM. To correct for radiation trapping effects, the fluorescence was excited and detected through a small pinhole placed in contact with the surface of the sample, following the method outlined in Ref. [38-39]. Several pinholes with diameters from 1.1 mm to 200 μm were used, and the lifetime of the detected fluorescence was calculated by fitting the temporal decay with a single exponential function (Eq. (11)).

$$I(t) = I_0 e^{(-t/\tau)} \tag{11}$$

Where I and I_0 are the fluorescence intensities at the time t and 0.

The actual lifetime was calculated as the extrapolation to null pinhole diameter of the decay times obtained with the different pinholes[38-39]. The resulting value of the upper level lifetime was 1.95 ms.

Fig. 8 shows the room temperature fluorescence decay curve of 5at% Yb:CaF_2 transparent ceramics obtained with a pinhole with 200 μm diameter. The small deviation from a pure single exponential decay is due to radiation trapping effects[39].

Finally, we tested the laser emission property of the sample. It was tested using the laser cavity layout shown in Fig. 9. The cavity is end pumped. The sample used in the experiments had a thickness of 1.5 mm and it was welded by a sheet of indium on a copper heat-sink and cooled by water at 19 ℃. The sample was pumped by a fiber-coupled laser-diode which emits at 929.4 nm with a Gaussian pump intensity distribution in the region of the focal plane (*i.e.* waist radius around 65 μm at $1/e^2$, measured with a CCD camera), numerical aperture of the pump beam 0.22. The other elements of the cavity are EM: End-Mirror, dichroic (high transmission for the pump wavelength, high reflection for the laser wavelength); FM: Folding-Mirror (spherical, ROC 100 mm);

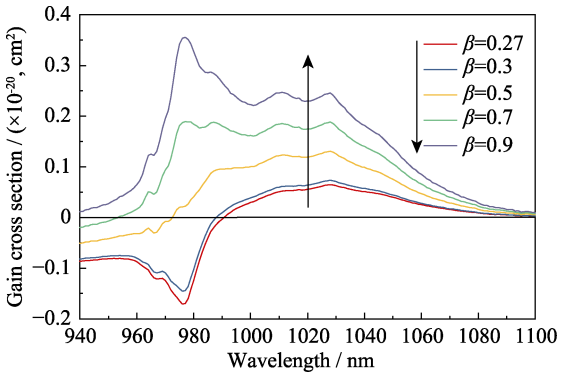

Fig. 7　The calculated gain cross section of 5at% Yb:CaF_2 ceramics

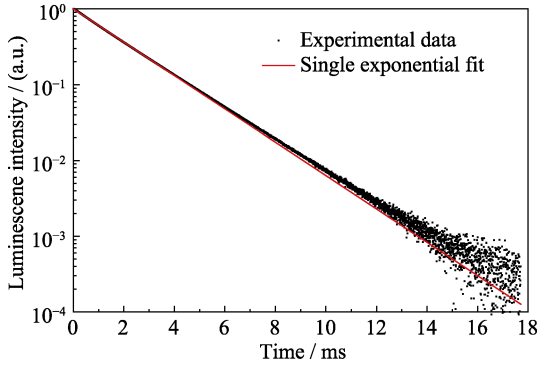

Fig. 8　The fluorescence decay curve of 5at% Yb:CaF_2 transparent ceramics at room temperature. The time constant τ of the fitting curve is 1.974 ms

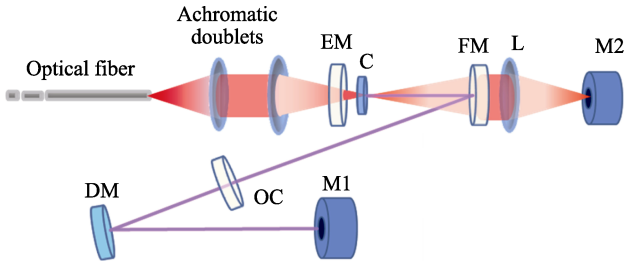

Fig. 9　Experimental set-up

OC: Flat Output Coupler mirror; M1 and M2: Power Meters, DM: Dichroic Mirror. The distance between EM and FM was 60 mm, while the distance between FM and OC was 270 mm.

The sample was pumped in Quasi-CW mode (QCW), with rectangular pump pulses at 10 Hz of repetition rate with a Duty Factor of DF=20%, in order to limit the thermal load into the sample. As the samples had different thickness and thus different absorption, the maximum incident pump power was adjusted to have about the same pump absorption for both samples. The sample absorbed about 14% of the incident pump, under lasing conditions. The maximum absorbed pump power was about 5 W for the sample (peak value during the pump on period), corresponding to about 38 W of incident pump power for the sample (peak values under the pump on period).

Several OC mirrors were used, with different values of transmission (from T_{oc}=2% to T_{oc}=12%), to find the optimal output coupling transmission.

The lasing wavelength was measured by means of a grating spectrometer equipped with a multichannel detector head, with a resolution of about 0.4 nm.

The graph of Fig. 10 shows the output power as a function of the absorbed pump power for the sample under test. The actual value of the absorbed pump power was assessed under lasing conditions, by means of the auxiliary power meter M2 shown in Fig. 9. The reported values of the pump and of the output power correspond to the value during the "on" period of the pump. For the sample, and in all the output coupling conditions the free running lasing wavelength is about 1028.5 nm. In QCW pumping conditions the maximum output power is 0.9 W, corresponding to an optical to optical efficiency η_O= 17.6%, obtained with a value of T_{oc}=7.2%. The maximum value of the slope efficiency is η_S=23.6% obtained with T_{oc}=12.4%. The main parameters of the laser emission are reported in Table 1.

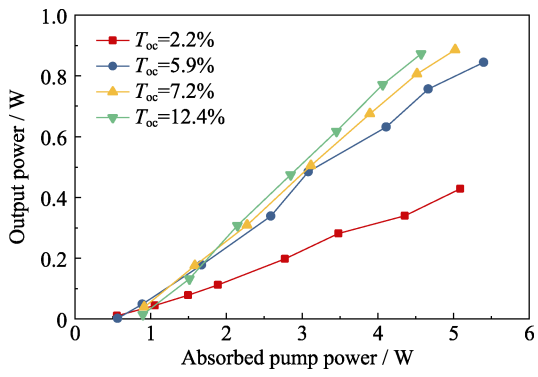

Fig. 10 Laser output power *vs*. incident pump power for different values of the output coupler mirror transmission T_{oc}

Table 1 Main laser emission parameters with slope efficiency being calculated with respect to the absorbed pump power

Output coupler transmission/%	Maximum power/W	Slope efficiency/%	Optical efficiency/%
2.2	0.429	9.6	8.4
5.9	0.845	18.2	15.6
7.2	0.886	21.2	17.6
12.4	0.874	23.6	19.1

3 Conclusion

In this work, 5at% Yb:CaF_2 transparent ceramics were successfully fabricated by vacuum sintering at 600 ℃ for 1 h and hot pressing post-treatment at 700 ℃ for 2 h from powders synthesized by the co-precipitation method. An effective washing process is necessary to remove some impurity ions in the powders. The used powders are pure cubic phase without secondary phase. The grain size of the powders is calculated to be 32 nm and the powders are agglomerated slightly. 5at% Yb:CaF_2 transparent ceramics have the homogeneous microstructure and the average grain size is about 360 nm. The in-line transmittance of the sample with the thickness of 1.5 mm reaches 92.0% at the wavelength of 1200 nm, which is close to the theoretical value. Furthermore, 5at% Yb:CaF_2 transparent ceramics have broad absorption and emission band. The strongest absorption and emission peaks are both at 977 nm. Meanwhile, the absorption cross section at 977 nm and the emission cross section at the 1030 nm of the ceramics are 0.39×10^{-20} and 0.26×10^{-20} cm^2, respectively. The lifetime of the $^5F_{5/2}$ level of the Yb^{3+} is 1.95 ms. In the laser experiment, the maximum slope efficiency of 23.6% and the maximum output power of 0.9 W under QCW pump conditions were obtained from the ceramics.

Reference:

[1] IKESUE A, AUNG Y L. Ceramic laser materials. *Nature Photonics*, 2008, **2(12):** 721–727.

[2] KRELL A, WAETZIG K, KLIMKE J. Influence of the structure of $MgO{\cdot}nAl_2O_3$ spinel lattices on transparent ceramics processing and properties. *Journal of the European Ceramic Society*, 2012, **32(11):** 2887–2898.

[3] FEDOROV P P, OSIKO V V, KUZNETSOV S V, *et al*. Fluoride laser nanoceramics. *Journal of Physics: Conference Series*, 2012, **345:** 012017.

[4] LUPEI V, LUPEI A, IKESUE A. Transparent polycrystalline ceramic laser materials. *Optical Materials*, 2008, **30(11):** 1781–1786.

[5] IKESUE A, KAMATA K. Microstructure and optical properties of hot isostatically pressed Nd: YAG ceramics. *Journal of the American Ceramic Society*, 1996, **79(7):** 1927–1933.

[6] LI JIANG, WU YU-SONG, PAN YU-BAI, *et al*. Fabrication, microstructure and properties of highly transparent Nd : YAG laser ceramics. *Optical Materials*, 2008, **31(1):** 6–17.

[7] LI JIANG, CHEN FENG, LIU WEN-BIN, *et al*. Co-precipitation synthesis route to yttrium aluminum garnet (YAG) transparent ceramics. *Journal of the European Ceramic Society*, 2012, **32(11):** 2971–2979.

[8] IKESUE A, AUNG Y L. Synthesis of Yb: YAG ceramics without sintering additives and their performance. *Journal of the American Ceramic Society*, 2017, **100(1):** 26–30.

[9] PIRRI A, ALDERIGHI D, TOCI G, *et al*. High-efficiency, high-power and low threshold Yb^{3+}: YAG ceramic laser. *Optics Express*, 2009, **17(25):** 23344–23349.

[10] MANGALARAJA R V, MOUZOM J, HEDSTROM P, *et al*. Combustion synthesis of Y_2O_3 and Yb-Y_2O_3 Part I. Nanopowders and their characterization. *Journal of Materials Processing Technology*, 2008, **208(1/2/3):** 415–422.

[11] KIM W, BAKER C, VILLALOBOS, *et al*. Synthesis of high purity Yb^{3+}-doped Lu_2O_3 powder for high power solid-state lasers. *Journal of the American Ceramic Society*, 2011, **94(9):** 3001–3005.

[12] ZHANG LEI, PAN WEI, FENG JING. Dependence of spectroscopic and thermal properties on concentration and temperature for Yb: Y_2O_3 transparent ceramics. *Journal of the European Ceramic Society*, 2015, **35(9):** 2547–2554.

[13] PIRRI A, TOCI G, PATRIZI B, *et al*. An overview on Yb-doped transparent polycrystalline sesquioxides laser ceramics. *IEEE Journal of Selected Topics in Quantum Electronics*, 2018, **24(5):** 1–8.

[14] TOCI G, PIRRI A, PATRIZI B, *et al*. High efficiency emission of a laser based on Yb-doped (Lu, $Y)_2O_3$ ceramic. *Optical Materials*, 2018, **83:** 182–186.

[15] LU XIAO, JIANG BEN-XUE, LI JIANG, *et al*. Synthesis of highly sinterable Yb: Sc_2O_3 nanopowders for transparent ceramic. *Ceramics International*, 2013, **39(4):** 4695–4700.

[16] BASIEV T T, DOROSHENKO M E, KONYUSHKIN V A, *et al*. Fluoride optical nanoceramics. *Russian Chemical Bulletin*, 2008, **57(5):** 877–886.

[17] AKCHURIN M S, BASIEV T T, DEMIDENKO A A, *et al*. CaF_2: Yb laser ceramics. *Optical Materials*, 2013, **35(3):** 444–450.

[18] AUBRY P, BENSALAH A, GREDIN P, *et al*. Synthesis and optical characterizations of Yb-doped CaF_2 ceramics. *Optical Materials*, 2009, **31(5):** 750–753.

[19] HATCH H E, PARSONS W F, WEAGLEY R J, *et al*. Hot-pressed polycrystalline CaF_2: Dy^{2+} laser. *Applied Physics Letters*, 2018, **5(8):** 153–154.

[20] SIEBOLD M, BOCK S, SCHRAMM U, *et al*. Yb: CaF_2 - a new old laser crystal. *Applied Physics B Lasers and Optics*, 2009, **97(2):** 327–338.

[21] HE YI-FENG, XUE YAN-YAN, LIU WEN-QIANG, *et al*. Structure and property of Yb doped $Ca_{1-x}R_xF_{2+x}$ (R= La, Gd) laser crystals. *Journal of Inorganic Materials*, 2017, **32(8):** 857–862.

[22] CARDINALI V, MARMOIS E, GARREC B, *et al*. Determination of the thermo-optic coefficient dn/dT of ytterbium doped ceramics (Sc_2O_3, Y_2O_3, Lu_2O_3, YAG), crystals (YAG, CaF_2) and neodymium doped phosphate glass at cryogenic temperature. *Optical Materials*, 2022, **34(6):** 990–994.

[23] TROPF W J. Temperature-dependent refractive-index models for BaF_2, CaF_2, MgF_2, SrF_2, LiF, NaF, KCl, ZnS, and ZnSe. *Optical Engineering*, 1995, **34(5):** 1369–1373.

[24] SIEBOLD M, HORNUNG M, BOEDEFELD R. Terawatt diode-pumped Yb: CaF_2 laser. *Optics Letters*, 2008, **33(23):** 2770–2772.

[25] SIEBOLD M, ROESER F, LOESER M, *et al*. PEnELOPE: a High Peak-power Diode-pumped Laser System for Laser-plasma Experiments. Conference on High-Power, High-Energy, and High-Intensity Laser Technology; and Research Using Extreme Light: Entering New Frontiers with Petawatt-Class Lasers, 2013, **8780:** 878005.

[26] LUCCA A, JACQUEMET M, DRUON F, *et al*. High-power tunable diode-pumped Yb^{3+}: CaF_2 laser. *Optics Letters*, 2004, **29(16):** 1879–1881.

[27] PIRRI A, ALDERIGHI D, TOCI G, *et al*. Direct comparison of Yb^{3+}: CaF_2 and heavily doped Yb^{3+}: YLF as laser media at room temperature. *Optics Express*, 2009, **17(20):** 18312–18319.

[28] PANG SI-YUAN, QIAN XIAO-BO, WU QING-HUI, *et al*. Structure and spectral property of Sc doped Nd: CaF_2 laser crystals. *Journal of Inorganic Materials*, 2018, **33(8):** 873–876.

[29] BASIEV T T, DOROSHENKO M E, FEDOROV P P, *et al*. Efficient laser based on CaF_2-SrF_2-YbF_3 nanoceramics. *Optics Letters*, 2008, **33(5):** 521–523.

[30] DUKEL'SKII K V, MIRONOV I A, DEMIDENKO V A, *et al*. Optical fluoride nanoceramic. *Journal of Optical Technology*, 2008, **75(11):** 728–736.

[31] LYBERIS A, PATRIARCHE G, GREDIN P, *et al*. Origin of light scattering in ytterbium doped calcium fluoride transparent ceramic for high power lasers. *Journal of the European Ceramic Society*, 2011, **31(9):** 1619–1630.

[32] LYBERIS A, STEVENSON A J, SUGANUMA A, *et al*. Effect of Yb^{3+} concentration on optical properties of Yb: CaF_2 transparent ceramics. *Optical Materials*, 2012, **34(6):** 965–968.

[33] KALLEL T, HASSAIRI M A, DAMMAK M, *et al*. Spectra and energy levels of Yb^{3+} ions in CaF_2 transparent ceramics. *Journal of Alloys and Compounds*, 2014, **584(7):** 261–268.

[34] LI WEI-WEI, MEI BING-CHU, SONG JING-HONG, *et al*. Yb^{3+} doped CaF_2 transparent ceramics by spark plasma sintering. *Journal of Alloys and Compounds*, 2016, **660:** 370–374.

[35] ABALLEA P, SUGANUMA A, DRUON F. Laser performance of diode-pumped Yb: CaF_2 optical ceramics synthesized using an energy-efficient process. *Optica*, 2015, **2(4):** 288–291.

[36] SARTHOU J, ABALLÉA P, PATRIARCHE G, *et al*. Wet-route synthesis and characterization of Yb: CaF_2 optical ceramics. *Journal of the American Ceramic Society*, 2016, **99(6):** 1992–2000.

[37] KITAJIMA S, YAMAKADO K, SHIRAKAWA A, *et al*. Yb^{3+}-doped CaF_2-LaF_3 ceramics laser. *Optics Letters*, 2017, **42(9):** 1724–1727.

[38] KÜHN H, FREDRICH-THORNTON S T, KRÄNKEL C, *et al*. Model for the calculation of radiation trapping and description of the pinhole method. *Optics Letters*, 2007, **32(13):** 1908–1910.

[39] TOCI G. Lifetime measurements with the pinhole method in presence of radiation trapping: I—theoretical model. *Applied Physics B*, 2012, **106(1):** 63–71.

[40] KRELL A, HUTZLER T, KLIMKE J, *et al.* Transmission physics and consequences for materials selection, manufacturing, and applications. *Journal of the European Ceramic Society*, 2009, **29(2):** 201–221.

[41] GUO YUE, LU SHUN-BIN, SU LIANG-BI, *et al*. Z-scan measurement of the nonlinear refractive index of Nd^{3+}, Y^{3+}-codoped CaF_2 and SrF_2 crystals. *Applied Optics*, 2015, **54(4):** 953–958.

[42] ITO M, GOUTAUDIER C, GUYOT Y, *et al*. Crystal growth, Yb^{3+} spectroscopy, concentration quenching analysis and potentiality of laser emission in $Ca_{1-x}Yb_xF_{2+x}$. *Journal of Physics: Condensed Matter*, 2004, **16:** 1501–1521.

共沉淀纳米粉体制备 Yb:CaF_2 激光陶瓷及其性能研究

韦家蓓 [1,2], TOCI Guido[3], PIRRI Angela[4], PATRIZI Barbara[5],
冯亚刚 [1,2], VANNINI Matteo[3], 李 江 [1, 2]

(1. 中国科学院 上海硅酸盐研究所, 透明光功能无机材料重点实验室, 上海 200050; 2. 中国科学院大学 材料科学与光电工程中心, 北京 100049; 3. 意大利国家研究委员会 国立光学研究所, 佛罗伦萨 50019; 4. 意大利国家研究委员会“Carrara”应用物理研究所, 佛罗伦萨 50019; 5. 意大利国家研究委员会 国立光学研究所, 比萨 56124)

摘 要: 利用共沉淀法合成的粉体, 通过真空烧结结合热压烧结后处理制备了掺镱的氟化钙透明陶瓷(Yb:CaF_2)。在 600 ℃预烧 1 h, 700 ℃热压烧结 2 h 制备的 5at%Yb:CaF_2 透明陶瓷在 1200 nm 处的直线透射率达到 92.0%。对陶瓷的显微结构、光谱特性和激光性能进行了测试和讨论。研究结果表明, 陶瓷样品的显微结构均匀, 平均晶粒尺寸为 360 nm。此外, 计算得到 Yb:CaF_2 陶瓷在 977 nm 处的吸收截面和 1030 nm 处的发射截面分别为 0.39×10^{-20} 和 0.26×10^{-20} cm^2。最后, 对 Yb:CaF_2 陶瓷激光性能进行了表征, 得到最大输出功率为 0.9 W, 最大斜率效率为 23.6%。

关 键 词: Yb:CaF_2; 共沉淀法; 两步烧结; 激光陶瓷; 光学性能

中图分类号: TQ174 **文献标识码:** A